Features of Flows past a Horizontal Plate in Stratified and Homogeneous Media

YULI D CHASHECHKIN[1], YAROSLAV ZAGUMENNYI[2]
[1]A.Yu. Ishlinskiy Institute for Problems in Mechanics of the RAS
101/1 prospect Vernadskogo, Moscow, 11926, RUSSIA
yulidch@gmail.com, chakin@ipmnet.ru
[2]Institute of Hydromechanics of the NASU
8/4 Zheliabova Street, 03680, Kyiv, UKRAINE
zagumennyi@gmail.com

Abstract: - Based on the fundamental system of equations a numerical approach is constructed for calculating in a single formulation various flows of strongly and weakly stratified fluids, which are typical for laboratory and environmental conditions, and potentially and actually homogeneous fluids, which are, respectively, physically valid and approximate mathematical models for "pure water" medium. The numerical method is developed in the framework of the open-source programming tools, OpenFOAM package, using high-order discretization schemes for all the derivatives in the governing equations and high spatial-temporal grid resolution of the computation domain. Unsteady flow patterns for the basic physical parameters, i.e. velocity, density, and pressure, and their derivatives, are studied around a thick and a thin rectangular horizontal plate for the fluid types under consideration. Comparison of the calculated velocity profiles and drag distribution on the surface of a horizontal plate with the Blasius solution for semi-infinite plane showed a strong influence of plate's thickness on the boundary layer flow structure and dynamics.

Key-Words: - Stratified medium, homogeneous fluid, horizontal plate, internal waves, vortices, numerical simulation, OpenFOAM

1 Introduction

Studies on flow past a plate oriented in the direction of free stream take an important place in hydrodynamics due to the fundamentality of the problem and importance of its practical applications. Although number of publications on the subject is very large, some earlier and recent problems are still not solved. Choice of shape and thickness of the leading edge of a straight wing is among the most important problems. It was thin in the aeronautical experiments by O. Liliental [1] and thick in the later airplane design by Right brothers [2], which had taken by that time a form similar to that in the modern aircrafts.

Nowadays, flows over a plate and a semi-infinite plane are studied extensively with purpose of improving the flow laminarization methods [3] and analyzing mechanisms for flow structuring and turbulence [4]. In this connection, a particular interest lies in construction of a theory on flows past obstacles, which enables calculating the physical parameters without introducing any additional constitutive hypotheses and relations with possibility of direct comparison with experiment.

Due to the mathematical complexity of the problem, researches started using different approximate models of flows past obstacles, such as the boundary layer theory [5], from the beginning of the 20-th century. The solution to the problem on flow over a half-plane, obtained under the assumption of a constant pressure in normal-to-wall direction [6], has been used for comparison with experiment and testing of numerical models [2, 7] for more than a hundred years. Later, the asymptotic methods for calculating homogeneous fluid and compressible gas flows in a wide range of velocities was proposed, which takes into account the edge effects [8] under the assumption of a complex multi-level flow structure over the surface. A state-of-the-art review on the boundary layer theory with account for its multi-level structure can be found in [9].

For calculating the vortex flow over a plate, the specific numerical schemes were developed, which simulate the separation and further reattachment of the boundary layer [10]. In the experiments of the recent years, the "streaky structures", which are transformed downstream into vortex systems with

further increase in velocity, were detected in the flow pattern over a flat surface [4, 11].

A new direction of the studies under consideration is associated with account for the stratification and diffusion effects. Taking the density variation into account in the system of equations makes it possible to calculate the flows structure and dynamics in a wide range of velocities [12]. In a quiescent non-equilibrium medium, flows compensating the deficiency of substance, caused by interruption of molecular transport of a stratifying agent, may arise even around a motionless impermeable obstacle [13].

The laboratory experiments have demonstrated that the fine structural elements in the diffusion-induced flows on a motionless obstacle do not disappear with the start of its motion but become even finer and more complicated. The fine structural elements are transformed into slow evolving high-gradient interfaces separating internal waves, vortices, and wakes [14].

The full asymptotic solution of the linearized problem using the singular perturbation methods contains two types of functions, including regularly perturbed ones, which describe the weakly attenuating internal waves, and singularly perturbed ones which describe the high-gradient interfaces near the obstacle and in the far field [15]. Analysis of the fundamental system of equations within a weak nonlinear approximation shows that the both large- and fine-scale flow components directly interact with each other [12]. The need for simultaneous calculation of the internal waves and the thin transverse streaky structures observed in the experiments [13, 16] impose strict demands on the mathematical models describing flows with account for the nonlinear effects.

With the development of computer systems and programming tools the mathematical modeling is set on a new level comparable under some criteria with laboratory experiment and full-scale observations in natural conditions. In the most papers, flows are calculated in the homogeneous fluid approximation [4, 7], including accounting for compressibility effects (barotropic media) [9]. At the same time, the search for solutions of the problem in the full formulation accounting for the baroclinicity, nonlinearity, and diffusion effects in a wide range of parameters is of a great scientific and practical interest [17].

In the present paper, the results on high performance computations of the flows around a uniformly moving plate oriented at a zero angle of attack in the both stratified and homogeneous viscous incompressible fluids are presented. The technique developed makes it possible to perform the computations within the single formulation in a wide range of plate lengths and velocities. Using the scale analysis of the system of equations [11], unsteady (transient) vortex regime is studied, which continues our previous studies on stratified flows around a motionless [13] and a uniformly moving horizontal plate in the linear approximation [15].

2 Problem Formulation

Mathematical modeling of the problem is based on the fundamental system of equation for multicomponent inhomogeneous incompressible fluid in the Boussinesq approximation. The buoyancy and diffusion effects of stratified components are taken into account, while the effects of heat-conductivity and heating due to dissipation are neglected [17, 12]. In the study of slow, as compared to the speed of sound, flows of fluids characterized by high thermal conductivity, one can account in calculations only for variations in density associated with concentration of the stratified component neglecting temperature variations. Thus, the governing equations take the following form

$$\begin{aligned} &\rho = \rho_{00}\left(\exp\left(-z/\Lambda\right)+s\right),\ \operatorname{div}\mathbf{v}=0,\\ &\frac{\partial \mathbf{v}}{\partial t}+\left(\mathbf{v}\nabla\right)\mathbf{v}=-\frac{1}{\rho_{00}}\nabla P+\nu\Delta\mathbf{v}-s\cdot\mathbf{g}, \qquad (1)\\ &\frac{\partial s}{\partial t}+\mathbf{v}\cdot\nabla s=\kappa_S\Delta s+\frac{\mathrm{v}_z}{\Lambda}. \end{aligned}$$

Here, s is the salinity perturbation including the salt compression ratio, $\mathbf{v}=\left(\mathrm{v}_x,\mathrm{v}_y,\mathrm{v}_z\right)$ is the vector of the induced velocity, P is the pressure except for the hydrostatic one, $\nu=10^{-2}\ \mathrm{cm}^2/\mathrm{s}$ and $\kappa_S=1.41\cdot10^{-5}\ \mathrm{cm}^2/\mathrm{s}$ are the kinematic viscosity and salt diffusion coefficients, t is time, ∇ and Δ are the Hamilton and Laplace operators respectively.

The proven solvability of the two-dimensional fluid mechanics equations enables calculating flows around obstacles for both strongly ($\Lambda=9.8$ m, $N=1\,\mathrm{s}^{-1}$, $T_b=6.28$ s) and weakly ($\Lambda=24$ km, $N=0.02\,\mathrm{s}^{-1}$, $T_b=5.2$ min) *stratified fluid*, and, as well, *potentially* ($\Lambda=10^8$ km, $N=10^{-5}\,\mathrm{s}^{-1}$, $T_b=7.3$ days) and *actually homogeneous* media ($\Lambda=\infty$, $N=0\ \mathrm{s}^{-1}$, $T_b=\infty$). In the case of

potentially homogeneous fluid density variations are so small that cannot be registered by existing technical instruments but the original mathematical formulation with the system of equations (1) is retained. In the case of *actually* homogeneous fluid the fundamental system of equations is degenerated on the singular components [12].

The experiments and calculations were carried out in two stages. Initially, an obstacle with impermeable boundaries is submerged with minimum disturbances into a quiescent stratified environment. Physically reasonable initial and boundary conditions in the associated coordinate system are no-slip and no-flux on the surface of the obstacle for velocity components and total salinity respectively, and vanishing of all perturbations at infinity.

Diffusion-induced flow is formed, which compensates interruption of the molecular transport of the stratifying agent on the obstacle [6]. The flow is then taken as the initial condition of the problem

$$\begin{aligned} &\mathbf{v},\, s,\, P\big|_{t\le 0} = \mathbf{v}_1(x,z),\;\; s_1(x,z),\;\; P_1(x,z), \\ &\mathrm{v}_x\big|_\Sigma = \mathrm{v}_z\big|_\Sigma = 0,\;\; \left[\frac{\partial s}{\partial \mathbf{n}}\right]\Big|_\Sigma = \frac{1}{\Lambda}\frac{\partial z}{\partial \mathbf{n}}, \\ &\mathrm{v}_x\big|_{x,\,z\to\infty} = U,\;\; \mathrm{v}_z\big|_{x,\,z\to\infty} = 0, \end{aligned} \qquad (2)$$

where, U, is the uniform free stream velocity at infinity, $\mathbf{n}$ is external normal to the surface, Σ, of the obstacle which can be either a plate or a wedge with length, L, and height, h, or, $2h$.

The set of equations and boundary conditions (1) – (2) are characterized by a number of parameters which contain length (Λ, L, h) or time $\left(T_b,\; T_U^L = L/U\right)$ scales and characteristics of the body motion or dissipative coefficients.

Large dynamic scales which are internal wave length, $\lambda = UT_b$, and viscous wave scale, $\Lambda_\nu = \sqrt[3]{g\nu}/N = \sqrt[3]{\Lambda\left(\delta_N^\nu\right)^2}$, characterize the attached internal wave fields structure [12, 18].

The flow fine structure is characterized by universal microscales, $\delta_N^\nu = \sqrt{\nu/N}$, $\delta_N^{\kappa_S} = \sqrt{\kappa_S/N}$, defined by the dissipative coefficients and buoyancy frequency, which are analogues of the Stokes scale on an oscillating surface, $\delta_\omega^\nu = \sqrt{\nu/\omega}$ [17]. Another couple of parameters such as Prandtl's and Peclet's scales are determined by the dissipative coefficients and velocity of the body motion, $\delta_U^\nu = \nu/U$ and $\delta_U^{\kappa_S} = \kappa_S/U$.

Relations of the basic length scales produce dimensionless parameters such as Reynolds, $\mathrm{Re} = L/\delta_u = UL/\nu$, internal Froude, $\mathrm{Fr} = \lambda/2\pi L = U/NL$, Péclet, $\mathrm{Pe} = L/\delta_\rho = UL/\kappa_S$, sharpness factor, $\xi_p = L/h$ or fullness of form, $\xi_S = S/Lh$, where S is the cross-sectional area of an obstacle, and, as well, relations specific for stratified media. The additional dimensionless parameters includes length scales ratio, $C = \Lambda/L$, which is the analogue of reverse Atwood number, $\mathrm{At}^{-1} = (\rho_1 + \rho_2)/(\rho_1 - \rho_2)$, for a continuously stratified fluid.

Such a variety of length scales with their significant differences in values indicates complexity of internal structure even of such a slow flow generated by small buoyancy forces which arise due to the spatial non-uniformity of molecular flux of the stratifying agent.

The large length scales prescribe size selection for observation or calculation domains which should contain all the studied structural components, such as upstream perturbations, downstream wake, internal waves, vortices, while the microscales determine grid resolution and time step. At low velocities of the body motion the Stokes scale is a critical one while at high velocities the Prandtl's scale is dominant.

3 Problem Solution

Solution for the system (1) with the boundary conditions (2) is constructed numerically using solvers, libraries, and other auxiliary utilities of own development in the framework of the open source computational package OpenFOAM based on the finite volume method. In order to account for the stratification and diffusion effects the standard *icoFoam* solver, which was initially constructed for solving the unsteady Navier–Stokes equations in the homogeneous fluid approximation, was supplemented with new variables including density ρ and salinity perturbation, s, and the corresponding equations for their calculation. New auxiliary parameters were also added, such as buoyancy frequency and scale, N, Λ, diffusion coefficient, κ_S, acceleration due to gravity, g, and others. The Navier–Stokes equation for vertical velocity component and the diffusion equation were supplemented with the terms characterizing effects

of buoyancy force and background stratification [19].

In order to interpolate the convective terms a limited TVD-scheme was used, which ensures minimal numerical diffusion and absence of solution oscillations. For discretization of the time derivative a second-order implicit asymmetric three-point scheme with backward differencing was used, which ensures a good time resolution of the physical process. For calculating the diffusion terms based on the Gauss theorem within orthogonal grid sections a surface normal gradient was evaluated at a cell face using a second order normal-to-face interpolation of the vector connecting the centers of the two neighbouring cells. . In non-orthogonal grid regions an iterative procedure with a user specified number of cycles was used for non-orthogonal correction of errors caused by a grid skewness.

For solving the resulting system of linear equations different iterative methods are used such as conjugate gradient method with PCG preconditioning applied to symmetric matrices and biconjugate gradient method with PBiCG preconditioning used for asymmetric matrices. As a preconditioner for symmetric matrices DIC procedure is chosen, which is based on a simplified procedure of incomplete Cholesky factorization. For asymmetric matrices, respectively, preconditioner DILU is used, which is based on a simplified incomplete LU factorization. For coupling equations for momentum and mass conservation a steady well-convergent algorithm PISO (Pressure-Implicit Split-Operator) is used, which works the most efficiently for transient problems.

The need for a high spatial resolution of the problem results in a quite large number of computational cells that makes it irrational performing computations on a single-processor computer. Decomposition of the computational domain for a parallel run is carried out by a simple geometric decomposition in which the domain is split into pieces by direction with an equal number of computational cells in each block. Such an approach allows setting a high spatial resolution of the computational domain and studying the problem in a wide range of the basic parameters for a quite reasonable time. The computations were performed in parallel using computing resources of the supercomputer “Lomonosov” of the Scientific Research Supercomputer Complex of MSU (SRCC MSU) and the technological platform UniHUB which provides direct access to the Joint Supercomputer Center Cluster of the RAS (JSCC RAS).

The calculations are terminated when the integral characteristics or their statistical evaluations take values of steady-state regime. The spatial dimensions of the computational cells are chosen from the condition of an adequate resolution of fine flow components associated with the stratification and diffusion effects, which impose significant restrictions on the minimal spatial step. In high-gradient regions of the flow at least several computational cells must fit the minimal linear scale of the problem. Calculation time step, Δt, is defined by the Courant’s condition, $\mathrm{Co} = |\mathbf{v}|\Delta t / \Delta r \le 1$, where Δr is the minimal size of grid cells and $\mathbf{v}$ is the local flow velocity. Additional control was ensured by comparison of independent calculations for fluids with different stratification.

4 Computation Results

The initial state of a non-equilibrium stratified medium near an impermeable obstacle is characterized by the diffusion-induced circulatory flows [13, 14]. A typical pattern of the vertical velocity component around the motionless impermeable horizontal plate in the exponentially stratified medium is shown in Fig.1a ($N = 1.2\ \mathrm{s}^{-1}$, $L = 10\ \mathrm{cm}$, $h = 0.5\ \mathrm{cm}$). For this figure and the following ones positive values of the visualized fields are colored green and negative ones are in blue color.

With start of uniform movement of the plate the diffusion-induced flow pattern with dissipative gravity waves manifested at the plate edges are changed drastically [20]. For all the velocities of the body motion the flow fields are characterized by a complicated internal structure. Around the slowly moving plate a group of attached waves with lengths, $\lambda = UT_b = 5.2\ \mathrm{cm}$, are formed in opposite phases at the plate edges (Fig.1b). Then, the main flow components become vortices which are formed around the leading edge of the plate and manifested downstream in the wake (Fig.1c). With further increase in velocity of the body motion the flow pattern becomes more and more non-stationary (Fig.1d).

Patterns of other fields have even more complicated fine structure. For comparison Fig.2 shows patterns of pressure and density gradients fields, as well as baroclinic vorticity generation and mechanical energy dissipation rates for both the strongly stratified and potentially homogeneous fluids.

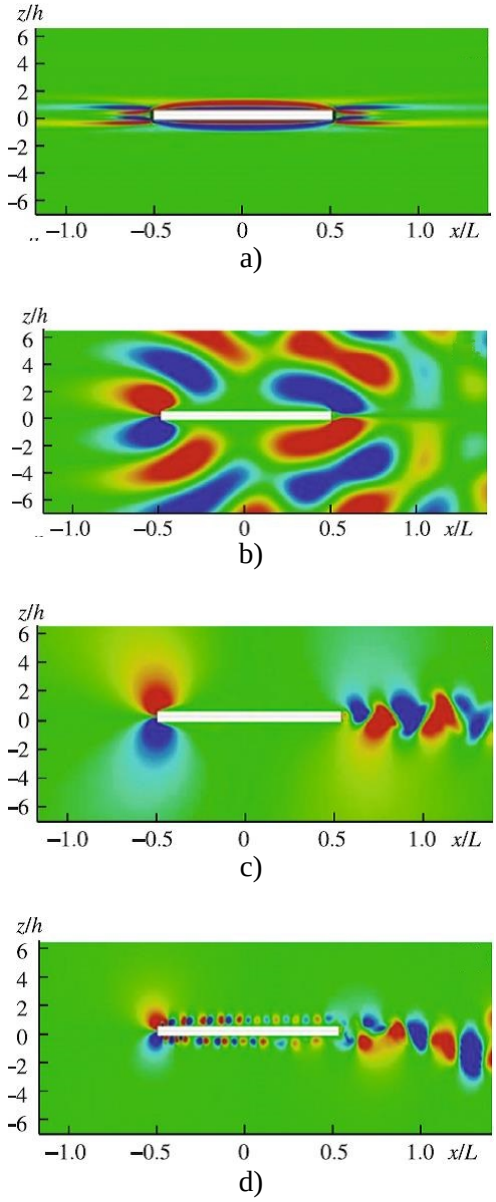

Fig.1. Patterns of the vertical component of velocity field around the horizontal plate ($L = 10$ cm, $h = 0.5$ cm) in stratified fluid ($N = 1.2\ \mathrm{s}^{-1}$): *a*) – diffusion-induced flow for $U = 0$; *b* - *d*) – $U =$ 1.0, 5.0, 80 cm/s, $\mathrm{Re} =$ 1000, 5000, 80000; $\lambda = UT_b$ = 5.2, 26, 418 cm.

Complexity of the patterns of the pressure and density gradients fields shown in Fig.2 is attributable to the properties of differential operators generating two groups of spots for each vortex core, which correspond to the regions of perturbation growth and attenuation respectively. At the same time, advantage of studying these patterns consists in a more complete visualization of the structural details, which makes it possible to identify small-scale elements against the background of larger elements.

The transverse dimensions of the flow components, which are determined by the values of kinetic coefficients in the given mathematical formulation, are minimal in the patterns of the density gradient fields. The pressure gradient fields are generally smooth, but close to the leading edge there are large variations due to the simultaneity of generation of the both large (internal waves, vortices) and fine flow components (Fig.2a, b).

In the pattern of the horizontal component of pressure gradient, $\partial P / \partial x$, (Fig.2a) a sequence of spots with different signs is manifested like in the vertical component of velocity field in Fig.2d, while the distribution of the vertical component of pressure gradient, $\partial P / \partial z$, shown in Fig.2b, demonstrates a more rarefied set of vertically oriented spots with different colors. Here, the vortices are well resolved and, in particular, there are ten cores above the plate, as it is seen from the patterns in Fig.2, which is greater by one than in case of the horizontal component of velocity field. Even a more complicate flow pattern is resolved near the leading edge. In the weakly stratified fluid, the perturbations degenerate more slowly as compared to that in the strongly stratified fluid and scales of the vortex structures are noticeably smaller.

The patterns of the component of density gradient are presented in Fig.2c, d. In the horizontal component of density gradient field thin layers with the both signs are localized on the vortex shells, which are combined in compact spots behind the body. In the weakly stratified fluid, the structures of the vertical component of density gradient are oriented mostly horizontally and form its own system of spiral curls typical for vortex elements. The local patterns of different physical variables in Fig.2c, d are substantially different, and locations of the centers of the regions which they outline do not coincide.

It should be specially noted the differences in the geometry and fine structure of the pressure and density gradients fields, which determine the spatial and temporal variations of such a dynamic parameter as the vorticity generation rate of the flow, and hence change in value of the vorticity itself.

Due to the differences in the spatial and temporal scales of the flow components, a general inhomogeneous distribution of the forces acting on the body, i.e. compression on the leading edge and stretch at the initial section of the side surface, is here supplemented with large variations in space and time. Further in the flow field pressure deficit zones (side stretching) are expressed due to the

passage of large vortices' centers which are the main sources of the side surface oscillation leading to development of such dangerous phenomena as buffeting and flutter. The difference in the fine details of the pressure gradient fields in the wake of the body is caused by the action of buoyancy forces suppressing fluid transfer in the vertical direction and the effects of the fine flow components.

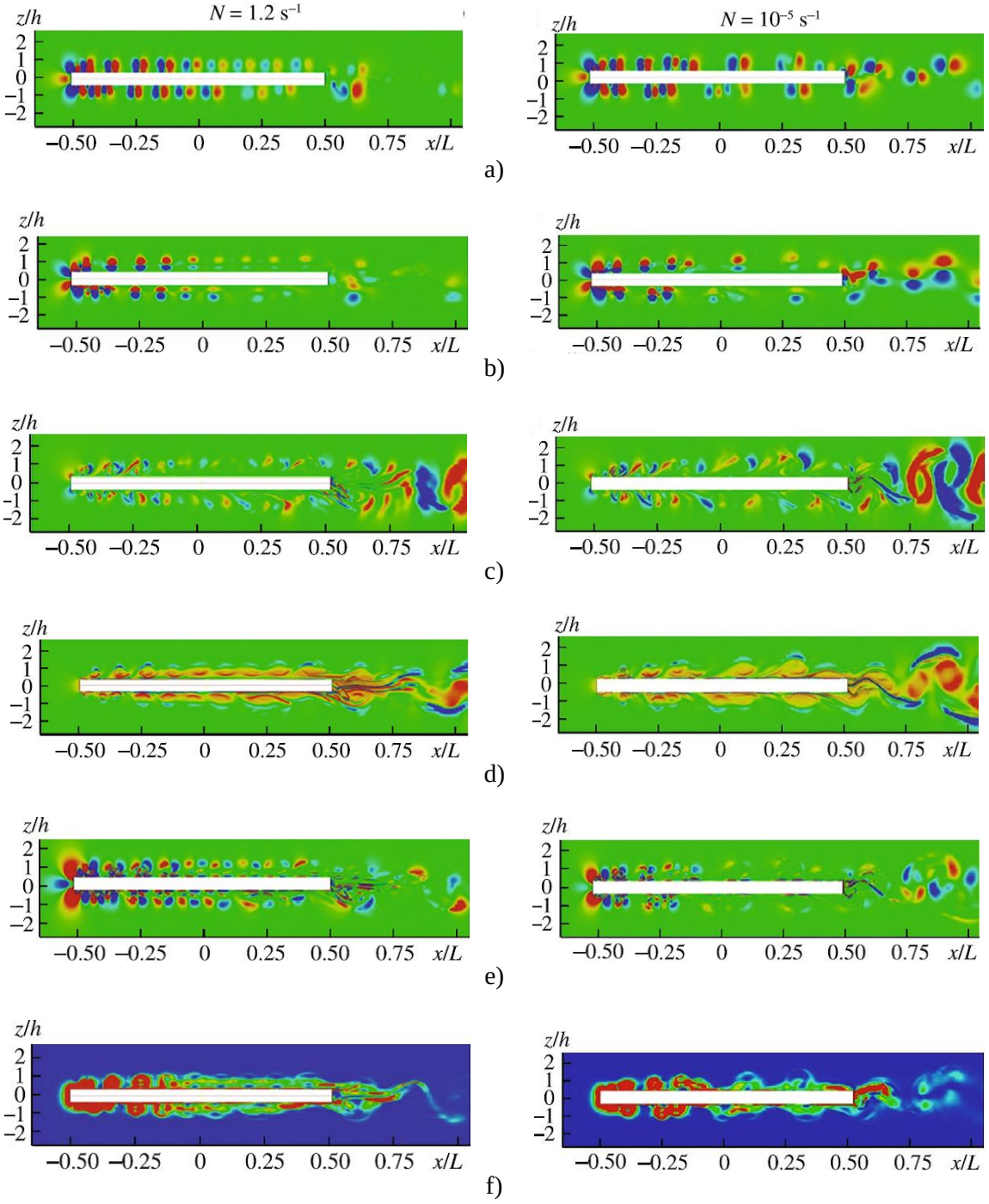

Fig.2. Calculated patterns of instantaneous fields around the plate ($L = 10$ cm, $h = 0.5$ cm, $U = 80$ cm/s) in the stratified (left column, $N = 1.2\ \mathrm{s}^{-1}$) and potentially homogeneous (right column, $N = 10^{-5}\ \mathrm{s}^{-1}$) fluids: *a*, *b*) – horizontal and vertical components of pressure gradient, *c*, *d*) – horizontal and vertical components of density gradient, *e)* – baroclinic vorticity generation rate, *f)* – mechanical energy dissipation rate.

There are two particular flow regions located exactly near the front and trailing edges of the plate where the main generation of vorticity vector, $\mathbf{\Omega} = \mathrm{rot}\,\mathbf{v}$, occurs, as a consequence of both the

overall reorganization of the velocity field and the baroclinic effects. Geometry of the density gradients field is complicated as the layered flow structure being developed downstream with distance from the leading edge. In the weakly stratified fluid range of oscillations of the vortices' size in the wake increases with distance from the trailing edge in the absence of stabilizing buoyancy forces.

Pattern of the spanwise component of the baroclinic vorticity generation rate, $d\boldsymbol{\Omega}/dt = \nabla P \times \nabla(1/\rho)$, is presented in Fig.2e, which is determined by the non-collinearity of pressure ∇P and density gradients $\nabla\rho$ according to the Bjerknes theorem. This field is the most complex and structured one in flows of inhomogeneous fluids. There are regions of its generation and dissipation with size of an order of the plate's thickness manifested above and below the front edge and in front of the body respectively. Further, downstream, the structures get thinner, and in addition to the remaining vortex elements a number of multiple thin zones of vorticity amplification and decay appear, which are gradually lengthened.

Fine linear structures are predominantly manifested in the wake behind the trailing edge of the plate, which are oriented mainly in the direction of the flow and deformed by the large irregularities. In the strongly stratified fluid the perturbations of the both signs are expressed along the whole length of the plate, but in the potentially homogeneous one they are only in the first quarter. There are regions of vorticity generation and dissipation manifested in the areas of interaction of the wake vortices with the free stream in the wake of the body. The geometry of the baroclinic vorticity generation rate field explains the formation dynamics of vortex flow fine structure and the mechanism for splitting of the fields into the layered structures observed in the schlieren images of the wake flows [12].

The mechanical energy dissipation rate field, $\varepsilon = 0.5\rho\nu\left(\partial\upsilon_i/\partial x_k + \partial\upsilon_k/\partial x_i\right)^2$, presented in Fig.2f, is different from zero in a relatively narrow zone in front of the body, where the horizontal flow turns, flowing the plate, and reaches maximal values in the vortex structures at the first third of the plate's length. Regions of dissipation observed at the second half of the plate are larger in the potentially homogeneous fluid than that for the strongly stratified one. It should be noted a qualitative difference in geometry of the vorticity generation rate field with its pronounced fine structures (Fig.2c) and a relatively smooth distribution of the energy dissipation rate field (Fig.2f).

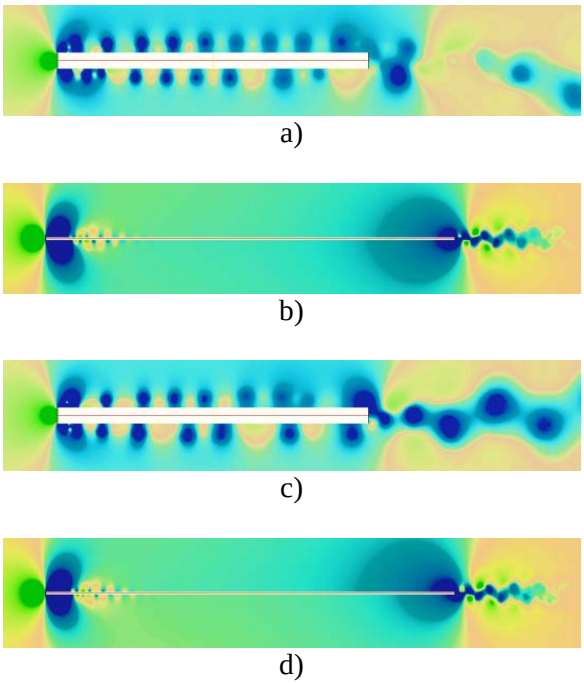

Fig.3. Patterns of the pressure field around the thick (*a*, *c* – h = 0.5 cm) and thin (*b*, *d* – h = 0.05 cm) horizontal plates ($L = 10$ cm , $U = 80$ cm/s):

a, *b*) – $N = 1.2\ \mathrm{s}^{-1}$; *c*, *d*) – $N = 0$

All the instantaneous flow patterns including the vorticity generation fields in Fig.2 are in a continuous evolution. The variation of the velocity pattern in the kinematic description is caused by the generation and break-up of new elements such as vortices due to the non-synchronized variation of the physical parameters with thermodynamic nature, in particular, the density and pressure gradients.

In the dynamic description, the generation of new elements with their own kinematics and spatial and temporal scales is associated with the high order and nonlinearity of the fundamental system of equations. Even in the linear approximation, the complete solutions of this system contain several functions, which can be treated in the nonlinear models as analogues of the components interacting with each other and generating new types of disturbances [12].

The pressure perturbation field shows a strong dependence on the transverse dimensions of the obstacle. In the wake past the thick plate, a number of large vortices develop (Fig.3a, b), while past the thin plate the transverse streaky structures are manifested (Fig.3c, d) similar to that observed in the experiment [14]. A more complete collection of flow patterns past the plates with different shapes are presented in [18].

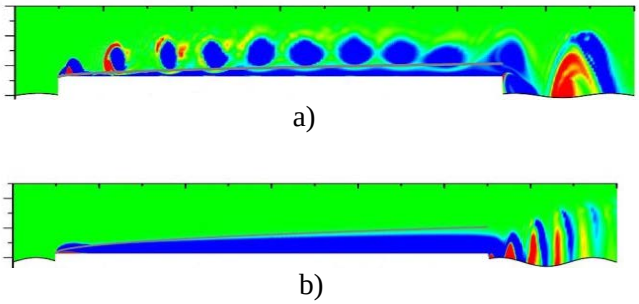

a)

b)

Fig.4. Patterns of the vorticity field over the thick ($a-$ h=0.5 cm) and thin ($b-$ h=0.05 cm) horizontal plates ($L=10$ cm , $U=80$ cm/s) in the potentially homogeneous fluid ($N=10^{-5}$ s^{-1}).

Calculations of flows around a thin and a thick horizontal plate in potentially homogeneous fluid at a transitional flow regime [18] show the vertical dimension of the obstacle has a strong influence on the fields structure that is observed in the experiments, as well [14]. The flow vortex structure depends essentially on the plate thickness in such a way that the vortices around the thick plate have a form of relatively large vortex filaments, while past the thin plate they look like a bundle of thin transverse streaks similar to those observed in the experiments [14].

Patterns of vorticity field, presented in Fig.4 for two values of the plate thickness, show the primary vorticity generation is localized around the leading and trailing edges of the plate, i.e. convergent and divergent flow regions where the primary processes of vortex structures formation and their further restructuring at transition to the wake flow occur. There is a sequence of sufficiently large vortex structures with anticyclonic rotation clearly manifested above the surface of the thick plate, which are partially wrapped with thin strips of vorticity with opposite sign.

There are a number of hardly distinguishable transverse structures near the leading edge of the thin plate (Fig.4), which rapidly attenuate downstream within the shear layer visualized in the vorticity field as a dark thickening strip adjacent directly to the surface. In the wake flow behind the thin plate streaky vortex elements are visualized, which decay downstream at a distance of about a quarter of the plate length. The gray lines in the vorticity field patterns denote the boundary layer based on the approximate Blasius solution for semi-infinite plane [6]. Away from the plate edges this curve outlines with a quite good accuracy the shear layer which in the case of the thick plate has a wavy structure due to interaction of the boundary layer with intense vortices during their drifting downstream in the outer flow region.

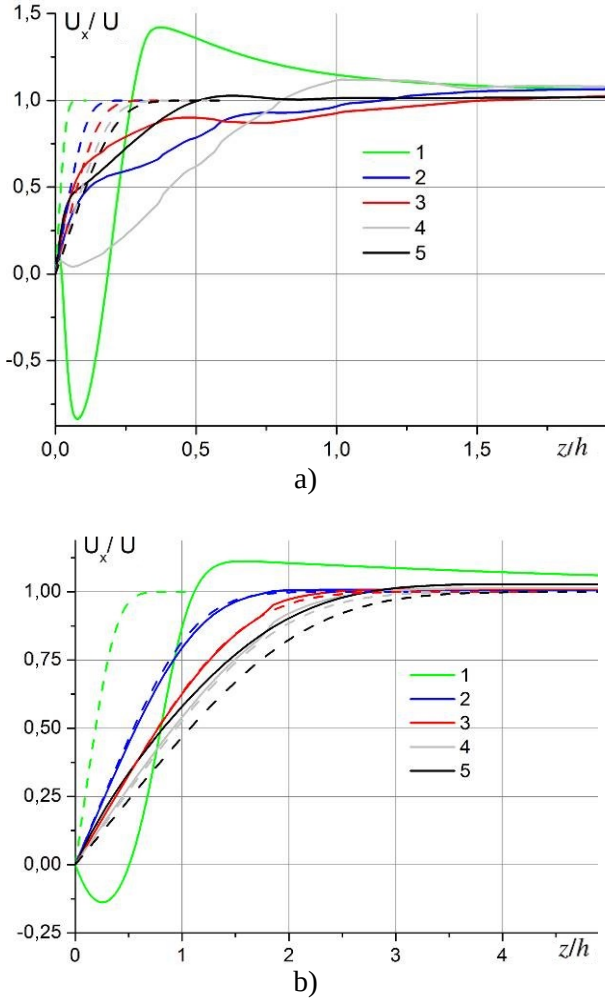

Fig.5. Velocity profiles in different cross sections on the thick (a - h=0.5 cm) and thin (b - h=0.05 cm) horizontal plates ($L=10$ cm , $U=80$ cm/s) in the potentially homogeneous fluid ($N=10^{-5}$ s^{-1}) in comparison with the Blasius solution [6] for semi-infinite plane (dash curves).

Velocity profiles at different cross sections on the thick plate, which are shown in Fig.5a, have quite a complex structure due to the effects of intense vortex dynamics. For this case, the calculated profiles substantially differ along the entire plate length from the corresponding curves obtained on the basis of the Blasius solution [6]. Quite a good agreement of the numerical and theoretical results is observed only in the flow region remote from the edges of the thin plate (Fig.5b). At the same time, within a distance from the plate edges less than a quarter of its length the

numerical and theoretical results are substantially different.

5 Conclusion

Based on the fundamental system of equations a numerical approach is constructed for calculating in a single formulation various flows of strongly and weakly stratified fluids, which are typical for laboratory and environmental conditions, and potentially and actually homogeneous fluids, which are, respectively, physically valid and approximate mathematical models for "pure water" medium.

Transformation of stratified flow structure is shown with increase in velocity of the body motion, starting from diffusion-induced flows generated by molecular flux breaking on an impermeable surface to non-stationary vortex flow regime at relatively high Reynolds numbers.

Unsteady patterns of the basic physical parameters, i.e. velocity, density, pressure, and their derivatives in the flow around a thick and a thin rectangular horizontal plate are studied for the fluid types under consideration.

The evolution of the individual structural elements is studied, both the general elements for all kinds of fluids and specific for stratified fluids, such as internal waves and thin layered interfaces. The physical mechanisms for vortex formation in the regions with high pressure and density gradients near the sharp edges are determined, and the dynamics of vortex interaction with the outer flow, violating the steady-state nature of the flow, are studied.

Comparison of the calculated velocity profiles and drag distribution on the surface of a horizontal plate with the Blasius solution for semi-infinite plane shows a strong influence of plate's thickness on the boundary layer flow structure and dynamics.

The flow around a plate with finite length in the general formulation is a complex physical process which requires a detailed experimental and theoretical study with account for the diffusion, heat conductivity, and compressibility effects, with the control of the criteria for observability and resolution of all the flow components with different scales.

References:

[1] O. Lilienthal, *Die Flugapparate, Algemeine Gesichtspunkte bei deren Herstellung und Anwendung*, Mayer and Muller, Berlin, 1894.

[2] W. Wright and O. Wright, *Pioneering Aviation Works of Wright Brothers*, http://www.paperlessarchives.com/wright brothers papers.htm

[3] R.E Hanson, H.P. Buckley, and P. Lavoie, Aerodynamic Optimization of the Flat Plate Leading Edge for Experimental Studies of Laminar and Transitional Boundary Layers, *Experiments in Fluids*, Vol.53, No.4, 2012, pp. 863-871.

[4] C. Liu, Y. Yan, and P. Lu, Physics of Turbulence Generation and Sustenance in a Boundary Layer, *Computers and Fluids*, Vol.102, 2014, pp. 353-384.

[5] L. Prandtl, Uber Flussigkeitsbewegung bei sehr kleiner Reibung, in: *Verhandlungen des III Internationalen Mathematiker-Kongress, Heidelberg, 1904*. Germany: Teubner, 1905, pp. 484-491.

[6] H. Schlichting, *Boundary Layer Theory*, Mc-Graw Hill, New York, 1968.

[7] T. Khapko, Y. Duguet, T. Kreilos, et al., Complexity of Localized Coherent Structures in a Boundary-Layer Flow, *Eur. Phys. J. E*, Vol.37, No.4, 2014, pp. 1-12.

[8] S. Goldstein, On Laminar Boundary-Layer Flow Near a Position of Separation, *Q. J. Mech. Appl. Math.* Vol.1, 1948, pp. 43-69.

[9] S. Braun and S. Scheichl, On Recent Developments in Marginal Separation Theory, *Phil. Trans. R. Soc.*, Vol.A372, No.2020, 2014, 20130343.

[10] A.M. Gaifullin and A.V. Zubtsov, Flow past a Plate with a Moving Surface, *Fluid Dynamics*, Vol.44, No.4, 2009, pp. 540-544.

[11] S.S. Sattarzadeh and J.H.M. Fransson, Experimental Investigation on the Steady and Unsteady Disturbances in a Flat Plate Boundary Layer, *Phys. Fluids*, Vol.26, 2014, 124103.

[12] Yu.D. Chashechkin, Differential Fluid Mechanics – Harmonization of Analytical, Numerical and Laboratory Models of Flows, *Mathematical Modeling and Optimization of Complex Structures*, Springer Series "Computational Methods in Applied Sciences", V.40, 2016, pp. 61-91.

[13] Ya.V. Zagumennyi and Yu.D. Chashechkin, Fine Structure of an Unsteady Diffusion-Induced Flow over a Fixed Plate, *Fluid Dynamics*, Vol.48, No.3, 2013, pp. 374-388.

[14] Yu.D. Chashechkin and V.V. Mitkin, A Visual Study on Flow Pattern around the Strip Moving Uniformly in a Continuously Stratified Fluid, *J. Visualiz.* Vol.7, No.2, 2004, pp. 127-134.

[15] R.N. Bardakov and Yu.D. Chashechkin, Calculation and Visualization of Two-Dimensional Attached Internal Waves in an Exponentially Stratified Viscous Fluid, *Izv. RAS, Fizika Atmos. Okeana*, 2004, Vol.40, No.4, pp. 531-544.

[16] R.N. Bardakov, V.V. Mitkin, and Yu.D. Chashechkin, Fine Structure of a Stratified Flow over a Plate, *Prikl. Mekh. Tekh. Fiz.*, Vol.48, No.6, 2007, pp. 77-91.

[17] L.D. Landau and E.M. Lifshits, *Theoretical Physics*. *V.6. Hydromechanics*, Pergamon Press, Oxford, 1987.

[18] Ya.V. Zagumennyi and Yu.D. Chashechkin, Pattern of Unsteady Vortex Flow around Plate under a Zero Angle of Attack (2D Problem), *Fluid Dynamics*, Vol.51, No.3, 2016, pp. 53-70.

[19] N.F. Dimitrieva and Ya.V. Zagumennyi, Numerical simulation of stratified flows using OpenFOAM package, *Proceedings of the Institute for System Programming RAS*, Vol.26, No.5, 2014, pp. 187-200.

[20] Yu.D. Chashechkin and Ia.V. Zagumennyi, Non-equilibrium processes in non-homogeneous fluids under the action of external forces, *Physica Scripta*, T155, 2013, paper 014010.